

Heterogeneous & Homogeneous & Bio- & Nano-

# CHEM **CAT** CHEM

---

CATALYSIS

## Accepted Article

**Title:** Highly Efficient Ru/MgO Catalyst with Surface-Enriched Basic Sites for Production of Hydrogen from Ammonia Decomposition

**Authors:** Ping Chen, Xiaohua Ju, Lin Liu, Xilun Zhang, Ji Feng, and Teng He

This manuscript has been accepted after peer review and appears as an Accepted Article online prior to editing, proofing, and formal publication of the final Version of Record (VoR). This work is currently citable by using the Digital Object Identifier (DOI) given below. The VoR will be published online in Early View as soon as possible and may be different to this Accepted Article as a result of editing. Readers should obtain the VoR from the journal website shown below when it is published to ensure accuracy of information. The authors are responsible for the content of this Accepted Article.

**To be cited as:** *ChemCatChem* 10.1002/cctc.201900306

**Link to VoR:** <http://dx.doi.org/10.1002/cctc.201900306>

# Highly Efficient Ru/MgO Catalyst with Surface-Enriched Basic Sites for Production of Hydrogen from Ammonia Decomposition

Xiaohua Ju,<sup>[a]</sup> Lin Liu,<sup>\*[a]</sup> Xilun Zhang,<sup>[a,b]</sup> Ji Feng,<sup>[a,b]</sup> Teng He,<sup>[a]</sup> Ping Chen<sup>\*[a]</sup>

Dedication ((optional))

**Abstract:** Development of highly active and stable catalyst for decomposition of ammonia to CO<sub>x</sub>-free hydrogen is an urgent and challenging task. Here, MgO (c-MgO) supported Ru nanoparticles derived from Ru/4MgCO<sub>3</sub>·Mg(OH)<sub>2</sub>·4H<sub>2</sub>O composite was prepared by deposition precipitation method and investigated as catalyst for NH<sub>3</sub> decomposition. The use of 4MgCO<sub>3</sub>·Mg(OH)<sub>2</sub>·4H<sub>2</sub>O as support precursor leads to high density of basic sites and highly dispersed Ru nanoparticles (3.8-6.0 nm) on the Ru/c-MgO catalysts. Thus, the Ru/c-MgO catalysts show much enhanced activities and robust stability in the long-term run (over 100 hours). Characterization results reveal that the much enhanced dispersion of Ru nanoparticles, high density of surface base sites and strong interaction between Ru nanoparticles and c-MgO all benefit the high efficient Ru/c-MgO catalysts in NH<sub>3</sub> decomposition. Further improvements in activity can be achieved by modification of Ru/c-MgO catalyst with an optimized KOH content. Therefore, it is believed that the use of 4MgCO<sub>3</sub>·Mg(OH)<sub>2</sub>·4H<sub>2</sub>O as support precursor opens opportunity to achieve highly active and stable Ru/MgO catalysts through tuning the basic properties of catalysts.

## Introduction

Hydrogen is one of the most promising energy carriers for the future energy systems, but the low volumetric energy density of hydrogen (in both compressed gas and liquid form) makes it difficult to store.<sup>[1]</sup> In recent years, ammonia, high gravimetric (17.7 wt.% H<sub>2</sub>), high volumetric H<sub>2</sub> density (121 kg H<sub>2</sub>/m<sup>3</sup> in the liquid form), high energy density (ca. 3 kWh/kg), liquid state under mild conditions (20°C and 0.8 MPa) and billion tons of annual production in world-wide, has attracted increasing attention as a promising carrier for hydrogen storage and transportation.<sup>[2]</sup> The CO<sub>x</sub>-free H<sub>2</sub> can be released via NH<sub>3</sub> decomposition reaction in presence of appropriate catalyst, which is a critical step for utilization of NH<sub>3</sub> as H<sub>2</sub> carrier for proton-exchange membrane fuel cells (PEMFC).<sup>[3]</sup> Thus, utilization of NH<sub>3</sub> as a feedstock offer a promising method for producing CO<sub>x</sub>-free H<sub>2</sub>, which is essential to build a more

sustainable society.

For catalytic NH<sub>3</sub> decomposition, supported Ru-based catalysts typically show high activity at relative low temperatures (400-500°C).<sup>[3g, 3i, 4]</sup> Up to now, a variety of supports, such as SiO<sub>2</sub>,<sup>[5]</sup> TiO<sub>2</sub>,<sup>[3i]</sup> zeolite,<sup>[5b]</sup> Al<sub>2</sub>O<sub>3</sub>,<sup>[6]</sup> MgO,<sup>[3i, 7]</sup> activated carbon,<sup>[3i, 8]</sup> carbon nanotubes,<sup>[3i, 3j, 9]</sup> and C12A7 electrides,<sup>[10]</sup> have been applied for Ru-based catalysts. Experimental observations reveal that the property of support is a critical factor for determining the catalytic activities of the supported Ru catalysts in NH<sub>3</sub> decomposition. Among the different Ru-based catalysts, Ru/MgO catalysts have received extensive attention for its high stability in NH<sub>3</sub> decomposition.<sup>[3i, 7]</sup> However, the activities of Ru/MgO catalysts obtained from different methods at relatively low temperature (< 450°C) still need to be improved due to the serious kinetic barrier.<sup>[11]</sup> As a basic metal oxide with suitable basic strength, MgO possesses ability to affect the geometric and electronic properties of supported Ru nanoparticles as a result of strong interaction between Ru nanoparticles and MgO support. The electron-donating ability of basic sites in MgO results in a significant positive influence on the metal-support interactions, and which is crucial for creation of highly active electron-rich Ru center. However, little attention has been paid to the influence of basic properties on the catalytic performances of Ru/MgO catalyst in NH<sub>3</sub> decomposition.

In this paper, we demonstrate that MgO supported Ru nanoparticles derived from Ru/4MgCO<sub>3</sub>·Mg(OH)<sub>2</sub>·4H<sub>2</sub>O composite (Ru/c-MgO) exhibits high catalytic activity and stability for NH<sub>3</sub> decomposition. The combination of Powder X-ray diffraction (XRD), Nitrogen-adsorption/desorption, transmission electron microscope (TEM), CO<sub>2</sub> temperature-programmed desorption (CO<sub>2</sub>-TPD), CO chemisorption, and H<sub>2</sub> temperature-programmed reduction (H<sub>2</sub>-TPR) techniques has been applied to study the effect of MgO support precursor on the physicochemical properties of Ru/c-MgO catalysts as well as their catalytic activities in NH<sub>3</sub> decomposition. It is proved that Ru/c-MgO catalysts which exhibit high density of basic sites can enhance the Ru dispersion and metal-support interaction, ultimately enhancing the activity and stability in NH<sub>3</sub> decomposition. Moreover, the influence of KOH modification on the activity and stability properties of Ru/c-MgO catalyst was also investigated.

## Results and Discussion

### Catalytic performance of Ru/c-MgO-DP catalysts

[a] X. Ju, Dr. L. Liu, X. Zhang, J. Feng, Dr. T. He, Prof. Dr. P. Chen  
Dalian National Laboratory for Clean Energy, State Key Laboratory of Catalysis  
Dalian Institute of Chemical Physics, Chinese Academy of Sciences  
Dalian, 116023, China  
E-mail: liulin@dicp.ac.cn  
pchen@dicp.ac.cn

[b] X. Zhang, J. Feng  
University of Chinese Academy of Sciences  
Beijing, 100049, China

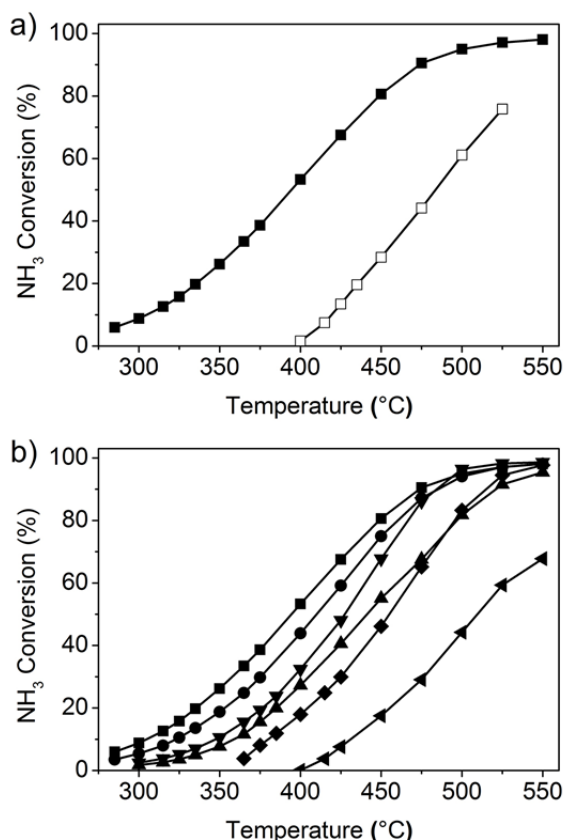


**Figure 1.** NH<sub>3</sub> conversion as a function of reaction temperature over Ru-based catalysts prepared from different supports: (a) 5%Ru/c-MgO-DP (■); 5%Ru/c-MgO-IM (□). (b) 5%Ru/c-MgO-DP (■); 3%Ru/c-MgO-DP (●); 1%Ru/c-MgO-DP (▲); 5%Ru/MgO-DP (▼); 5%Ru/Al<sub>2</sub>O<sub>3</sub>-DP (◆); 5%Ru/SiO<sub>2</sub>-DP (◄).

Figure 1a shows the temperature dependence of NH<sub>3</sub> conversion for Ru/c-MgO catalysts prepared by deposition precipitation method (DP) and impregnation method (IM). It can be seen that the preparation methods have a great influence on the catalytic performances of the Ru/c-MgO catalysts. The 5%Ru/c-MgO-DP exhibits much higher catalytic activity than the 5%Ru/c-MgO-IM in the temperature ranging from 300–550°C (Figure 1a), manifesting the importance of preparation method for the formation of highly active catalysts. The 5%Ru/c-MgO-DP readily shows apparent activity starting from 300°C, while 5%Ru/c-MgO-IM displays negligible activity at temperature below 400°C. The NH<sub>3</sub> conversion of 5%Ru/c-MgO-DP is 2.8 times that of 5%Ru/c-MgO-IM at 450°C, and 5.0 times that of 5%Ru/c-MgO-IM at 425°C. For the 5%Ru/c-MgO-DP sample, only a very small amount of chlorine species (0.1 wt%) were included in the reduced sample. However, a large amount of chlorine (1.0 wt%) still remained in 5%Ru/c-MgO-IM even after the sample was calcined and reduced at 550°C. The chlorine species have negative effect for 5%Ru/c-MgO-IM catalysts, and should partially responsible for its relatively low activity.

To evaluate the influence of supports on the catalytic performances of supported Ru catalysts, Ru catalysts supported on the conventional oxides such as MgO, SiO<sub>2</sub>, and Al<sub>2</sub>O<sub>3</sub> were

also prepared with DP method and tested for NH<sub>3</sub> decomposition. For the catalysts with similar Ru content, the activities follow the order of 5%Ru/c-MgO-DP > 5%Ru/MgO-DP > 5%Ru/Al<sub>2</sub>O<sub>3</sub>-DP > 5%Ru/SiO<sub>2</sub>-DP (Figure 1b). The NH<sub>3</sub> conversion of 5%Ru/c-MgO-DP can reach 80.6% at 450°C, which is much higher than that of the 5%Ru/MgO-DP (67.7%), 5%Ru/Al<sub>2</sub>O<sub>3</sub>-DP (46.1%), and 5%Ru/SiO<sub>2</sub>-DP samples (17.5%). Above results clearly show that the use of 4MgCO<sub>3</sub>·Mg(OH)<sub>2</sub>·4H<sub>2</sub>O for the preparation of Ru/c-MgO-DP catalyst is critical in achieving high catalytic activity. The activity of 3%Ru/c-MgO-DP catalyst is about 75.0% at 450°C, which is also higher than that of the 5%Ru/MgO-DP, 5%Ru/Al<sub>2</sub>O<sub>3</sub>-DP and 5%Ru/SiO<sub>2</sub>-DP at the same temperature. Remarkably, not only the 5%Ru/c-MgO-DP but also the 3%Ru/c-MgO-DP and 1%Ru/c-MgO-DP have much higher activity than that of the 5%Ru/Al<sub>2</sub>O<sub>3</sub>-DP and 5%Ru/SiO<sub>2</sub>-DP catalysts. At 450°C, the NH<sub>3</sub> conversion of 1%Ru/c-MgO can reach 55.0%, while the NH<sub>3</sub> conversion of 5%Ru/Al<sub>2</sub>O<sub>3</sub>-DP and 5%Ru/SiO<sub>2</sub>-DP catalysts are only about 46.1% and 17.5%, respectively. Above results clearly indicated that 4MgCO<sub>3</sub>·Mg(OH)<sub>2</sub>·4H<sub>2</sub>O is an more effective support precursor to prepare highly efficient catalysts than the conventional oxide supports such as MgO, SiO<sub>2</sub> and Al<sub>2</sub>O<sub>3</sub>.

A comparison of activity of Ru/c-MgO-DP catalysts with those of the other efficient Ru-based catalysts for NH<sub>3</sub> decomposition reported in literatures is listed in Table 1. The NH<sub>3</sub> conversion of 5%Ru/c-MgO-DP is superior to most of the unmodified supported Ru catalysts in literatures. The calculation of H<sub>2</sub> formation rate of catalyst per gram was based on the weight of the reduced Ru/c-MgO catalyst. It can be found that the 3%Ru/c-MgO-DP and 1%Ru/c-MgO-DP catalysts also possess much higher H<sub>2</sub> formation rate than most of Ru-based catalysts under similar reaction condition. Considering the amount of Ru content in 1%Ru/c-MgO-DP catalysts, the H<sub>2</sub> formation rate of catalyst per gram Ru is 4.3 times that of typical efficient 5%Ru/MgO-DP catalyst at same reaction condition.

In addition, their catalytic behavior of 3%Ru/c-MgO-DP was further examined with a supply of pure ammonia at various gas hour space velocity (GHSV) values (2,000–30,000 mL/g<sub>cat</sub>·h). Figure 2a depicts effect of GHSV on the catalytic performance of 3%Ru/c-MgO-DP catalyst. It can be seen that NH<sub>3</sub> conversion at the reaction temperature of 300–500°C decreases remarkably with increase of GHSV because of the increase in the residence time of the reactants. At the temperature of 400°C, nearly complete conversion can be obtained with a GHSV as high as 2,000 mL/g<sub>cat</sub>·h.

The long-term stability is critical for evaluating the catalytic performance of catalyst in NH<sub>3</sub> decomposition (Figure 2b). At a relatively high space velocity of 30,000 mL/g<sub>cat</sub>·h, the catalytic activity of 3%Ru/c-MgO-DP was tested at 500°C. Quite impressively, no deterioration of the catalytic activity was observed for 110 hours. Thus, the stability of the Ru/c-MgO-DP catalyst is firmly established as the conversion remained at ~93% level almost constant over a relatively long period of time. Here, Ru/c-MgO-DP catalyst not only gives high activity but also gives high stability, demonstrating the great potential for the application as efficient catalyst in NH<sub>3</sub> decomposition reaction.

**Table 1.** NH<sub>3</sub> conversion over supported Ru catalysts at 450°C (GHSV: 30,000 mL/g<sub>cat</sub>·h).

Catalyst	Method	Ru loading (wt %)	NH <sub>3</sub> conversion (%)	H <sub>2</sub> formation rate (mmol/g <sub>cat</sub> min)	H <sub>2</sub> formation rate (mol/g <sub>Ru</sub> min)	Reference
Ru/Al <sub>2</sub> O <sub>3</sub>	IM <sup>a</sup>	10	31.5	11.5	0.12	[9]
Ru/SiO <sub>2</sub>	IM <sup>a</sup>	10	34.5	11.4	0.11	[9]
Ru/CNTs	IM <sup>b</sup>	4.8	43.3	14.5	0.30	[16]
Ru/MgO	IM <sup>b</sup>	4.8	30.8	10.3	0.22	[16]
Ru/TiO <sub>2</sub>	IM <sup>b</sup>	4.8	27.2	9.1	0.19	[16]
Ru/Al <sub>2</sub> O <sub>3</sub>	IM <sup>b</sup>	4.8	23.3	7.8	0.16	[16]
Ru/AC	IM <sup>b</sup>	4.8	28.7	9.6	0.20	[16]
Ru/MgO	Polyol reduction	2.8	41.3	13.8	0.49	[28]
Ru/MgO	DP	3.5	56.5	18.9	0.54	[29]
Ru/MgO	DP	5.0	67.7	22.7	0.48	This work
Ru/c-MgO	DP	0.9	55.0	18.4	2.09	This work
Ru/c-MgO	DP	2.9	75.0	25.1	0.89	This work
Ru/c-MgO	DP	4.7	80.6	27.0	0.60	This work

[a] Prepared by wetness incipient impregnation with water as solvent. [b] Prepared by wetness incipient impregnation with acetone as solvent.

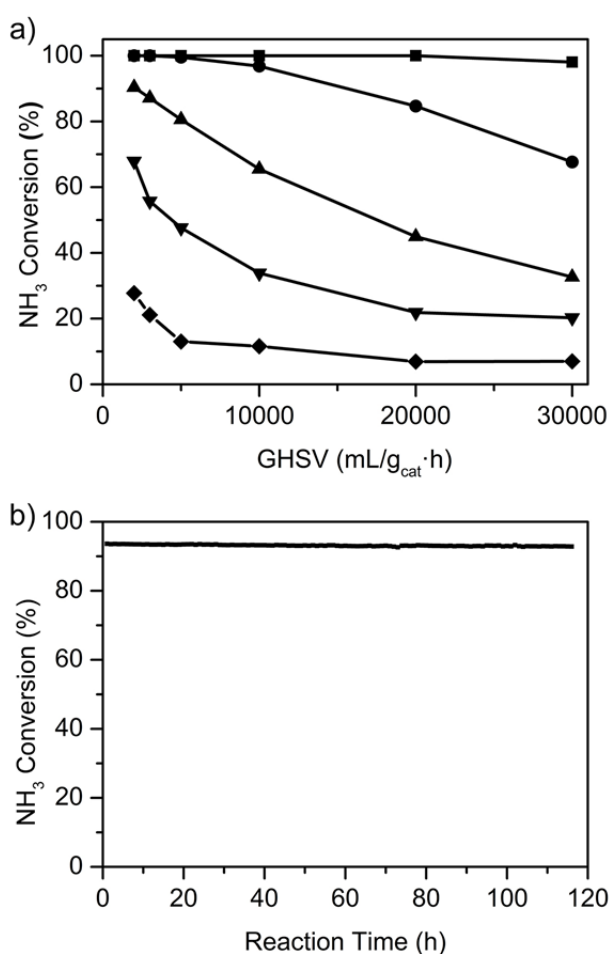


**Figure 2.** (a) Effect of GHSV on the catalytic performance of 3%Ru/c-MgO-DP catalyst for NH<sub>3</sub> decomposition at different temperature: 500°C (■); 450°C (●); 400°C (▲); 350°C (▼); 300°C (◆). (b) Stability of 3%Ru/c-MgO-DP catalyst for NH<sub>3</sub> decomposition at 500°C.

### Structure characterization of the Ru/c-MgO-DP catalysts

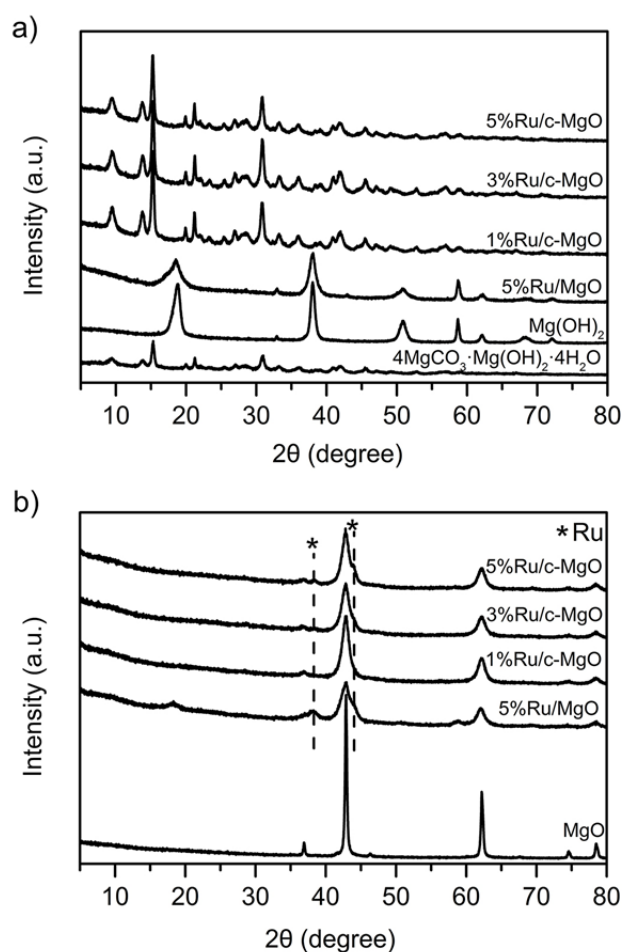


**Figure 3.** XRD patterns of as-prepared (top) and reduced (bottom) 5%Ru/MgO-DP, 1%Ru/c-MgO-DP, 3%Ru/c-MgO-DP, and 5%Ru/c-MgO-DP. 4MgCO<sub>3</sub>·Mg(OH)<sub>2</sub>·4H<sub>2</sub>O, Mg(OH)<sub>2</sub>, and MgO were also included for a comparison.

The structures of the samples before and after reaction were investigated by powder XRD. Figure 3 shows XRD patterns of the as-prepared and reduced Ru/MgO samples prepared from different supports. For the as-prepared Ru/MgO-DP sample,

only diffraction peaks corresponding to  $\text{Mg}(\text{OH})_2$  phase can be observed, indicating the conversion of  $\text{MgO}$  into  $\text{Mg}(\text{OH})_2$  during the preparation process. In comparison with that of  $\text{Ru}/\text{MgO}$ -DP sample, a remarkable difference can be observed for the as-prepared  $\text{Ru}/\text{c-MgO}$ -DP samples. Only peaks corresponding to the  $4\text{MgCO}_3 \cdot \text{Mg}(\text{OH})_2 \cdot 4\text{H}_2\text{O}$  phase can be observed in the XRD pattern of  $\text{Ru}/\text{c-MgO}$ -DP samples with different Ru contents, indicating the structure of  $4\text{MgCO}_3 \cdot \text{Mg}(\text{OH})_2 \cdot 4\text{H}_2\text{O}$  retained after preparation. For all the reduced  $\text{Ru}/\text{c-MgO}$ -DP and  $\text{Ru}/\text{MgO}$ -DP samples, only diffraction peaks corresponding to  $\text{MgO}$  can be observed, which reveals the decomposition of  $\text{Mg}(\text{OH})_2$  and

$4\text{MgCO}_3 \cdot \text{Mg}(\text{OH})_2 \cdot 4\text{H}_2\text{O}$  into  $\text{MgO}$  after reduction (Figure 3a). In the XRD pattern of the reduced 5% $\text{Ru}/\text{MgO}$ -DP sample, the weak and broad peaks (at Bragg angles of 38.4, 42.2 and 44.0°) diffraction features attributable to metallic Ru can be identified, indicating the crystal size of Ru particles was big enough to be detected by XRD. For the reduced  $\text{Ru}/\text{c-MgO}$ -DP samples, no diffraction features attributable to metallic Ru can be observed for the sample with a low Ru content of 1%. For the reduced  $\text{Ru}/\text{c-MgO}$ -DP samples with a higher Ru content, besides the diffraction lines of  $\text{MgO}$  support, small and broad peaks corresponding to Ru metal can also be observed.

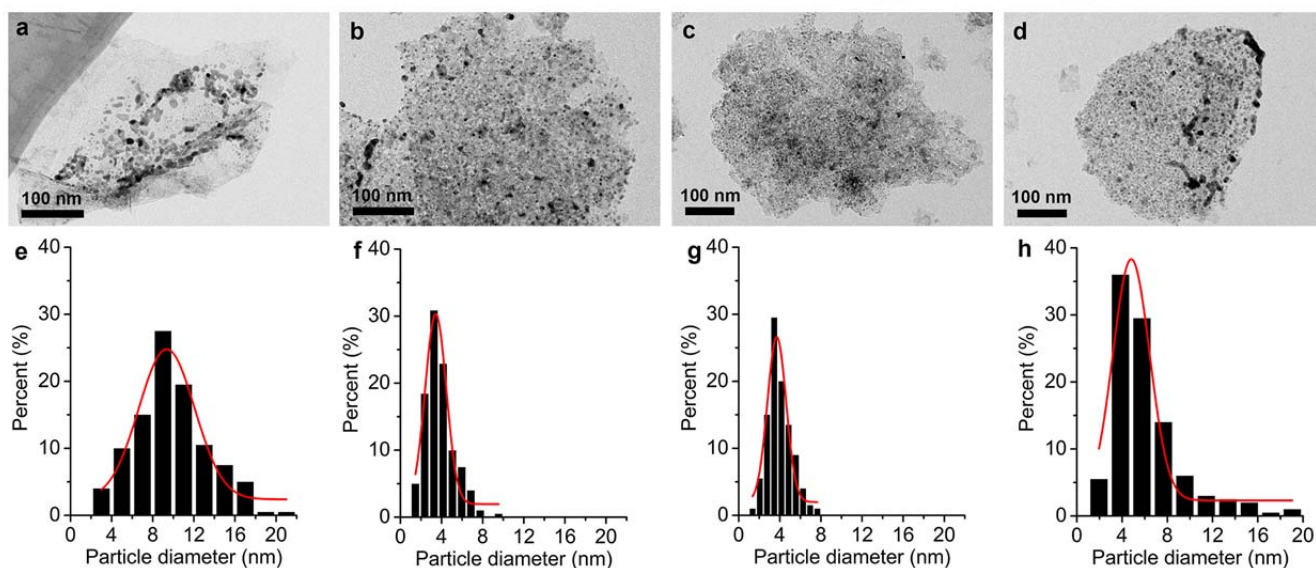


**Figure 4.** TEM images and corresponding Ru particle size distributions of 5% $\text{Ru}/\text{MgO}$ -DP (a and e), 1% $\text{Ru}/\text{c-MgO}$ -DP (b and f), 3% $\text{Ru}/\text{c-MgO}$ -DP (c and g), and 5% $\text{Ru}/\text{c-MgO}$ -DP (d and h).

**Table 2.** Properties of  $\text{Ru}/\text{MgO}$ -DP and  $\text{Ru}/\text{c-MgO}$ -DP samples.

Sample	Surface area ( $\text{m}^2/\text{g}$ )	Ru particle size by TEM (nm)	Metal dispersion by CO chemisorption (%)	Ru particle size by CO chemisorption (nm)
5% $\text{Ru}/\text{MgO}$ -DP	283.6	9.8	12.8	10.5
1% $\text{Ru}/\text{c-MgO}$ -DP	47.7	3.8	37.1	3.6
3% $\text{Ru}/\text{c-MgO}$ -DP	53.2	3.9	38.7	3.5
5% $\text{Ru}/\text{c-MgO}$ -DP	51.0	6.0	21.1	6.4

The influence of support on the particle size distribution and morphology of dispersed Ru nanoparticles was studied by TEM. The metal particle size of the reduced catalyst is shown in the TEM images in Figure 4. It can be seen that loading of Ru on the surface of  $4\text{MgCO}_3 \cdot \text{Mg}(\text{OH})_2 \cdot 4\text{H}_2\text{O}$  leads to the formation of highly dispersed Ru nanoparticles on the support. The particle size distribution and average diameter of Ru nanoparticles for the reduced 5% $\text{Ru}/\text{MgO}$ -DP and  $\text{Ru}/\text{c-MgO}$ -DP samples with different Ru contents can be estimated by measuring around 200 particles randomly taken from TEM images. Quantitatively, the average metal particle sizes of 1% $\text{Ru}/\text{c-MgO}$ -DP, 3% $\text{Ru}/\text{c-}$

$\text{MgO}$ -DP and 5% $\text{Ru}/\text{c-MgO}$ -DP are 3.8, 3.9 and 6.0 nm, respectively, which are much smaller than that of reduced 5% $\text{Ru}/\text{MgO}$ -DP sample (9.8 nm). The 1% $\text{Ru}/\text{c-MgO}$ -DP and 3% $\text{Ru}/\text{c-MgO}$ -DP catalysts have similar metal particle size. For the  $4\text{MgCO}_3 \cdot \text{Mg}(\text{OH})_2 \cdot 4\text{H}_2\text{O}$  support, plenty of hydroxyl and carbonate groups on the surface allow the  $\text{Ru}^{3+}$  ions to be adsorbed. In fact, almost all of the  $\text{Ru}^{3+}$  ions can be adsorbed on the surface of  $4\text{MgCO}_3 \cdot \text{Mg}(\text{OH})_2 \cdot 4\text{H}_2\text{O}$  as evidenced by the colorless of the solution after stirring for 1 h. The surface adsorbed  $\text{Ru}^{3+}$  ions can be precipitated and deposited as highly dispersed Ru precursor species ( $\text{RuO}_x(\text{OH})_y$ ,  $\text{RuO}_2 \cdot 2\text{H}_2\text{O}$ , or  $\text{Ru}(\text{OH})_x$ ) on the surface of  $4\text{MgCO}_3 \cdot \text{Mg}(\text{OH})_2 \cdot 4\text{H}_2\text{O}$  along with the release of  $\text{NH}_3$  from hydrolysis of urea during the preparation process. In the following reduction process, highly dispersed Ru nanoparticles can be formed on the surface of c-MgO support which come from the decomposition of  $4\text{MgCO}_3 \cdot \text{Mg}(\text{OH})_2 \cdot 4\text{H}_2\text{O}$ . In comparison with  $\text{Ru}/\text{MgO}$ -DP sample, the plenty of basic sites of c-MgO support derived from  $4\text{MgCO}_3 \cdot \text{Mg}(\text{OH})_2 \cdot 4\text{H}_2\text{O}$  can enhance the interaction between Ru species and c-MgO supports, which can induce the much enhanced dispersion of Ru nanoparticles on the surface of c-MgO support. Therefore,

loading of Ru on the  $4\text{MgCO}_3 \cdot \text{Mg}(\text{OH})_2 \cdot 4\text{H}_2\text{O}$  support leads to much enhanced dispersion of Ru in comparison with that of the MgO support, which should account for the remarkably increased catalytic activity of Ru/c-MgO-DP samples for  $\text{NH}_3$  decomposition.

Ru catalyzed  $\text{NH}_3$  decomposition has been demonstrated to be a structural sensitive reaction, and the activity of Ru-based catalyst can be greatly influenced by the dispersion, size and morphology of Ru nanoparticles.<sup>[12]</sup> To further study the influence of Ru dispersion on the catalytic performance of the 5%Ru/MgO-DP and Ru/c-MgO-DP samples, CO chemisorption was also applied to determine the Ru dispersion. From Table 2, it can be seen that the use of  $4\text{MgCO}_3 \cdot \text{Mg}(\text{OH})_2 \cdot 4\text{H}_2\text{O}$  as support precursor has a significantly influence on the dispersion degree of Ru nanoparticles. According to the CO chemisorption results, the Ru dispersion value of 5%Ru/c-MgO-DP is about 21.1%, which is larger than that of the 5%Ru/MgO-DP with same Ru loading (12.8%). The Ru particle size of 5%Ru/c-MgO-DP catalysts estimated by CO chemisorption was about 6.4 nm, which is consistent with the value obtained from TEM results (~6.0 nm). The CO chemisorption results also show that the Ru content has a notable impact on the Ru dispersion of Ru/c-MgO-DP samples, and Ru/c-MgO-DP samples with low Ru content induces a much enhanced Ru dispersion. Consistent with the catalytic activity results, both TEM and CO chemisorption results reveal that the use of  $4\text{MgCO}_3 \cdot \text{Mg}(\text{OH})_2 \cdot 4\text{H}_2\text{O}$  as support precursor induces a much enhanced dispersion of Ru on the surface of Ru/c-MgO-DP samples.

The  $\text{H}_2$  formation rate per gram Ru of the Ru/MgO catalysts calculated to reveal the intrinsic catalytic activities of the Ru/MgO catalysts studied. It can be found that the Ru/c-MgO-DP catalysts possess higher  $\text{H}_2$  formation rate in comparison with that of 5%Ru/MgO-DP catalyst in the temperature range of 350-500°C (Figure 5a). Among the Ru/c-MgO-DP catalysts with different Ru contents, the  $\text{H}_2$  formation rates follow the order of 1%Ru/c-MgO-DP > 3%Ru/c-MgO-DP > 5%Ru/c-MgO-DP. The  $\text{H}_2$  formation rate of 1%Ru/c-MgO-DP catalyst is 0.29 mol/(g<sub>Ru</sub>·min), 3.9 times that of typical 5%Ru/MgO-DP catalyst at 350°C, while the  $\text{H}_2$  formation rate of 1%Ru/c-MgO-DP was 4.3 times that of 5%Ru/MgO-DP at 450°C. Above results clearly show that the apparent high activity of Ru/c-MgO-DP in comparison with that of the Ru/MgO-DP catalyst.

The  $\text{H}_2$  formation turnover frequency ( $\text{TOF}_{\text{H}_2}$ ), which can be calculated by on the  $\text{H}_2$  formation rate to the number of exposed Ru surface atoms per gram of catalyst, has been used as a standard parameter for the evaluation of intrinsic catalytic performance of different catalyst. Figure 5b shows that the  $\text{TOF}_{\text{H}_2}$  values of Ru/c-MgO-DP and Ru/MgO-DP catalysts all increase with the increase of reaction temperature. In the temperature range of 400-550°C. Among the different Ru/MgO-DP catalysts with different Ru contents, the TOF values follow the order of 1%Ru/c-MgO-DP > 5%Ru/MgO-DP > 3%Ru/c-MgO-DP. At 500°C, the 1%Ru/c-MgO-DP displays a significantly  $\text{TOF}_{\text{H}_2}$  of 9.5 s<sup>-1</sup>, which is not only much higher than that of 5%Ru/MgO-DP (6.3 s<sup>-1</sup>), but also outperforms 3%Ru/c-MgO-DP (3.9 s<sup>-1</sup>) and 5%Ru/c-MgO-DP (4.8 s<sup>-1</sup>) catalyst under similar condition. However, a much different order

can be observed in the relatively reaction temperature ranging from 300 to 350°C. The TOF values follow the order of 5%Ru/c-MgO-DP > 1%Ru/c-MgO-DP > 3%Ru/c-MgO-DP > 5%Ru/MgO-DP. Above results clearly show that both the composition of the catalysts and reaction temperature can influence the intrinsic activity of Ru/MgO-DP catalysts. It worthy of mentioning that  $\text{NH}_3$  synthesis, a rise in TOF over promoted Ru/Al<sub>2</sub>O<sub>3</sub> and AC-supported Ru catalysts has been observed with the increase of size of Ru particles.<sup>[12a, 12b]</sup> It has been found that  $\text{NH}_3$  decomposition on supported Ru catalysts is also highly structure sensitive, with  $\text{TOF}_{\text{H}_2}$  values increasing by almost 2 orders of magnitude as the particle size increases from 0.8 nm to >7 nm.<sup>[12c]</sup> Herein, the  $\text{TOF}_{\text{H}_2}$  values of 5%Ru/c-MgO-DP catalyst also shows obvious decrease in comparison with 5%Ru/MgO-DP with larger particle size, which agrees well with the previous reported Ru/MgO catalyst systems in  $\text{NH}_3$  decomposition.<sup>[12]</sup> For the Ru/c-MgO-DP catalysts with Ru loading of 1 wt.% and 3 wt.%, similar Ru dispersion value and Ru particle size can be obtained. However, remarkable different  $\text{TOF}_{\text{H}_2}$  value can be observed for the 1%Ru/c-MgO-DP and 3%Ru/c-MgO-DP. In comparison with 3%Ru/c-MgO-DP, much enhanced  $\text{TOF}_{\text{H}_2}$  value can be observed on 1%Ru/c-MgO-DP in the temperature range or 300-500°C. For example, the 1%Ru/c-MgO-DP give much higher  $\text{TOF}_{\text{H}_2}$  values of 9.4 s<sup>-1</sup> than that of the 3%Ru/c-MgO-DP (3.8 s<sup>-1</sup>) at 450°C. Decomposition on Ru is known to be structure-sensitive reactions as a result of highly dependence of active B5 sites on the particle size and shape. In a Ru/Al<sub>2</sub>O<sub>3</sub> system, both experimental results and theoretical results show that the number of active B5 sites is highly dependent on particle shape and increases with particle size up to 7 nm for flat nanoparticles. The maximum TOF (based on total exposed Ru atoms) and number of active B5 sites occur at ~7 nm for elongated nanoparticles compared to at ~1.8-3 nm for hemispherical nanoparticles.<sup>[12c]</sup> Here, both the Ru dispersion value and Ru particle size are average values estimated from the highly dispersed Ru particles with different sizes and irregular morphologies. Thus, the remarkable difference in the  $\text{TOF}_{\text{H}_2}$  values of 1%Ru/c-MgO-DP and 3%Ru/c-MgO-DP should mainly arise from the obvious difference in the particle size distribution and morphology of non-uniform Ru nanoparticles on the c-MgO surface.

The textural properties of Ru/c-MgO-DP samples were studied by N<sub>2</sub> sorption. Figure 6 shows N<sub>2</sub> adsorption/desorption isotherms of the reduced 5%Ru/MgO-DP and Ru/c-MgO-DP samples with different Ru contents. The reduced 5%Ru/MgO-DP exhibits type IV isotherms with H3 hysteresis as defined by the IUPAC. The hysteresis loops in the relative pressure P/P<sub>0</sub> between 0.5 and 1.0 indicates the presence of uniform mesopores in the reduced 5%Ru/MgO-DP, which is consistent with our previous report. The BET surface areas of reduced 5%Ru/MgO-DP and Ru/c-MgO-DP samples with different Ru contents are summarized in Table 2. Table 2 shows the specific surface area, average Ru particle size (estimated by TEM and CO-chemisorption), and Ru dispersion of the four Ru-based catalysts. It can be seen that the 5%Ru/MgO-DP has a high surface area of 283.6 m<sup>2</sup>/g, which is not only larger than that of the MgO derived  $4\text{MgCO}_3 \cdot \text{Mg}(\text{OH})_2 \cdot 4\text{H}_2\text{O}$  (142.6 m<sup>2</sup>/g), but also

larger than that of the Ru/c-MgO-DP samples with different Ru contents ( $\sim 50 \text{ m}^2/\text{g}$ ). Generally a higher surface area of support produces higher Ru dispersion. However, 5%Ru/MgO-DP which has the highest surface area only gives a lowest Ru dispersion. Thus, the surface areas of the catalysts may not be the key factor in causing the difference of the Ru dispersions and catalytic performances of 5%Ru/MgO-DP and Ru/c-MgO-DP catalysts studied here.

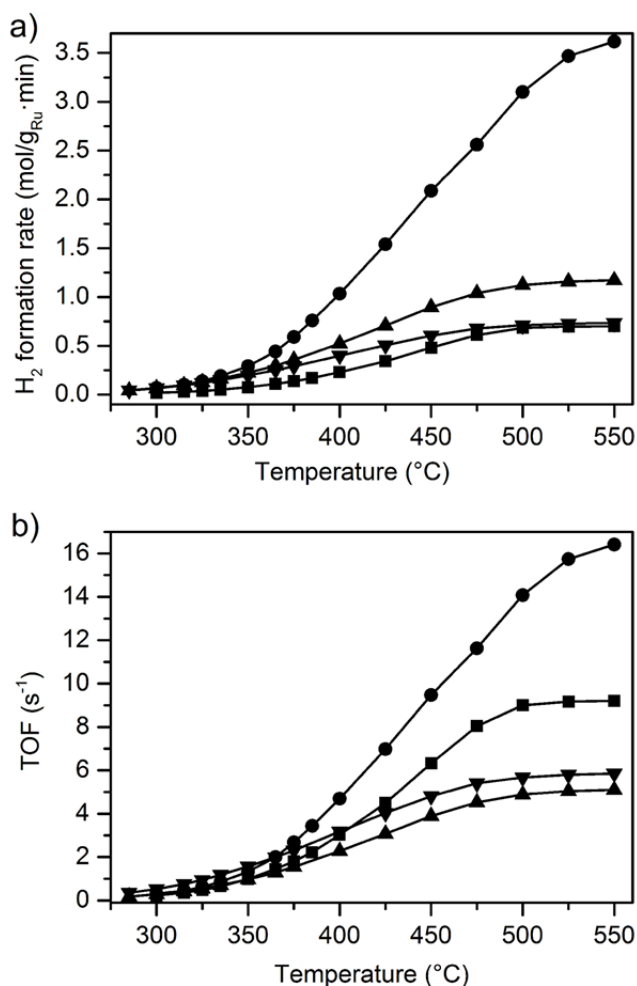


**Figure 5.**  $\text{H}_2$  formation rate (a) and  $\text{TOF}_{\text{H}_2}$  (b) as a function of reaction temperature on different Ru-based catalysts: 5%Ru/MgO-DP (■); 1%Ru/MgO(C)-DP (●); 3%Ru/MgO(C)-DP (▲); 5%Ru/MgO(C)-DP (▼).

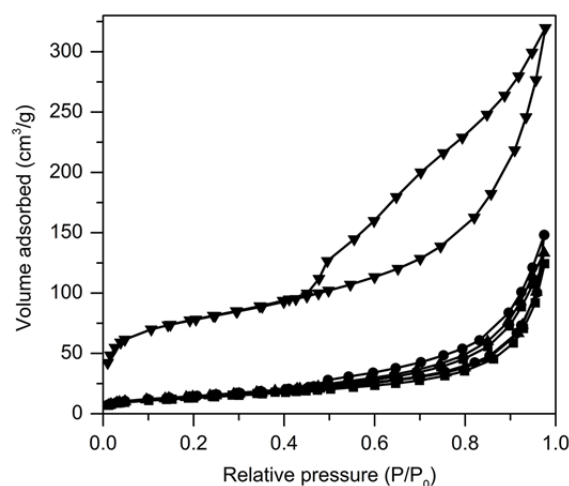


**Figure 6.**  $\text{N}_2$  sorption isotherms of reduced 5%Ru/MgO-DP (▼), 1%Ru/c-MgO-DP (■), 3%Ru/c-MgO-DP (●), and 5%Ru/c-MgO-DP (▲).

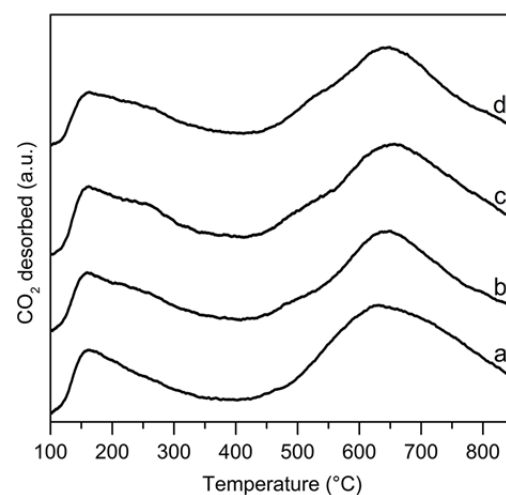


**Figure 7.**  $\text{CO}_2$ -TPD spectra of reduced 5%Ru/MgO-DP (a), 1%Ru/c-MgO-DP (b), 3%Ru/c-MgO-DP (c), and 5%Ru/c-MgO-DP (d).

**Table 3.** Basic properties of 5%Ru/MgO-DP and Ru/c-MgO-DP samples

sample	Peak temperature (°C)	Quantity ( $\text{cm}^3/\text{g}$ )	Surface area ( $\text{m}^2/\text{g}$ )	Density of basic sites ( $\mu\text{mol}/\text{m}^2$ )
5%Ru/MgO-DP	162.1	23.8	283.6	3.7
	630.7	55.6	283.6	8.8
1%Ru/c-MgO-DP	159.6	29.4	47.7	27.5
	648.5	57.8	47.7	54.1
3%Ru/c-MgO-DP	161.4	29.7	53.2	24.9
	656.9	54.7	53.2	45.9
5%Ru/c-MgO-DP	162.6	25.1	51.1	22.0
	649.4	56.0	51.1	49.0

The CO<sub>2</sub>-TPD measurement was conducted to examine the basic property of the 5%Ru/MgO-DP and Ru/c-MgO-DP samples. Figure 7 displays the CO<sub>2</sub> desorption profiles of 5%Ru/MgO-DP and Ru/c-MgO-DP with different Ru contents in the temperature range of 100-800°C. Similar with that of the 5%Ru/MgO-DP sample, the Ru/c-MgO-DP samples with different Ru contents also show similar desorption peaks at ca. 160 and 650°C respectively. The density of basic sites on the 5%Ru/MgO-DP and Ru/c-MgO-DP samples as calculated by the integral method based on the area of the corresponding samples. As shown in Table 3, the high temperature (ca. 650°C) basic density of Ru/c-MgO-DP samples are in the range of 45-54 μmol/m<sup>2</sup>, about 5-6 times that of 5%Ru/MgO-DP (8.8 μmol/m<sup>2</sup>). Note also that the Ru/c-MgO-DP samples give much higher density of low temperature (ca. 160°C) basic sites than that of the 5%Ru/MgO-DP sample. These profiles suggest that the Ru/c-MgO-DP samples possess significantly enhanced density of surface basic sites, which may account for the much enhanced NH<sub>3</sub> decomposition activity of Ru/c-MgO-DP samples.

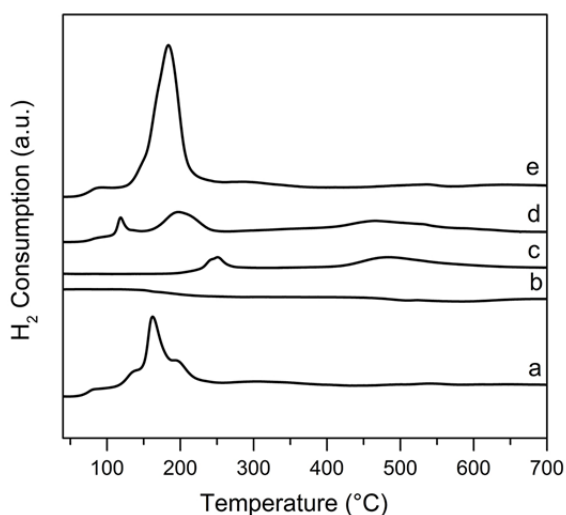


**Figure 8.** TPR profiles of (a) 5%Ru/MgO-DP, (b) c-MgO, (c) 1%Ru/c-MgO-DP, (d), 3%Ru/c-MgO-DP, and (e) 5%Ru/c-MgO-DP.

H<sub>2</sub>-TPR experiments were also carried out to reveal the origin of remarkable difference in the catalytic activities of Ru/MgO-DP and Ru/c-MgO-DP samples. To exclude the influence of other reaction (e.g. methanation) and desorbed species (e.g. H<sub>2</sub>O, CO<sub>2</sub>, CH<sub>4</sub>) on the determination of H<sub>2</sub> consumption, the Ru/c-MgO-DP samples were firstly treated at 450°C for 2 h, which can convert the 4MgCO<sub>3</sub>·Mg(OH)<sub>2</sub>·4H<sub>2</sub>O support precursor into MgO as proved by XRD (Figure S2) and TG-DTG results (Figure S3). Thus, the detected peaks during the TPR testing detected by TCD detector can be attributed to the consumption of H<sub>2</sub> during the reduction of Ru precursor species. For a comparison, the TPR profile of 4MgCO<sub>3</sub>·Mg(OH)<sub>2</sub>·4H<sub>2</sub>O treated at 450°C for 2 h was also recorded. As shown in Figure 8, no H<sub>2</sub> consumption peaks can be observed from the TPR profiles of the 4MgCO<sub>3</sub>·Mg(OH)<sub>2</sub>·4H<sub>2</sub>O treated at 450°C. For 5%Ru/MgO-DP

sample, the onset reduction temperature is at about 60°C, and several broad reduction peaks with peak temperatures at about 90, 130, 160, and 195°C can be observed. The presence of several broad reduction peaks in the temperature range of 60-200°C clearly reveals the interaction between different kinds of Ru species with MgO support in 5%Ru/MgO-DP sample. The onset reduction temperature of 5%Ru/c-MgO-DP is also at about 60°C, which is similar with that of the 5%Ru/MgO-DP sample. Different from that of 5%Ru/MgO-DP sample, only a broad peak at ca. 187°C can be observed for 5%Ru/c-MgO-DP sample. Decrease of Ru loading amount from 5% to 1% resulted in a remarkable difference in the TPR spectra of Ru/c-MgO-DP samples. Besides a broad peak at temperature below 300°C, an additional broad peak centered at about 460-480°C appeared for the 3%Ru/c-MgO-DP and 1%Ru/c-MgO-DP sample. As the Ru/c-MgO-DP sample with different Ru content were obtained from same method, the remarkable difference in the reduction behavior should be highly related to the differences of metal-support interaction induced by the high density basic sites. Some of weakly interacted Ru species with the support could be easily reduced, while strongly interacted Ru species with the support could only be reduced at much improved temperature. With the decrease of Ru loading, both the low temperature (150-300°C) and high temperature reduction peak (400-600°C) of Ru/c-MgO-DP showed a tendency to move to the higher temperatures, indicating much enhanced interaction between Ru species and MgO support in Ru/c-MgO-DP. The TPR results show the positive role of high density of basic sites in promoting the strong metal-support interaction in Ru/c-MgO-DP samples, which may also beneficial for the enhancement of catalytic activity.

#### Kinetic test of Ru/MgO-DP catalysts

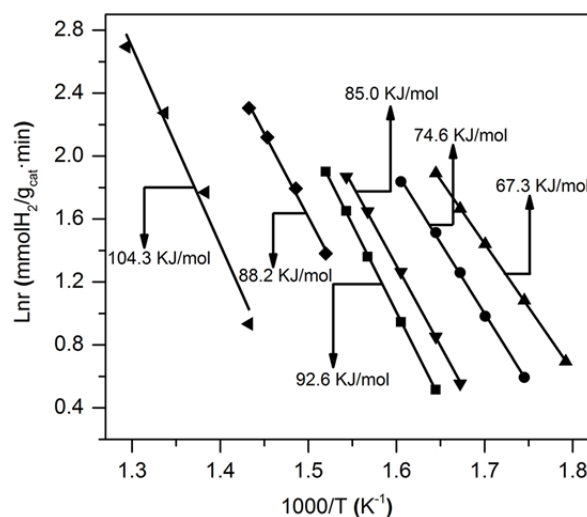


**Figure 9.** Arrhenius plots of the supported Ru catalysts: 1%Ru/c-MgO-DP (■); 3%Ru/c-MgO-DP (●); 5%Ru/c-MgO-DP (▲); 5%Ru/MgO-DP (▼); 5%Ru/Al<sub>2</sub>O<sub>3</sub>-DP (◆); 5%Ru/SiO<sub>2</sub>-DP (◄).

Based on  $\text{NH}_3$  conversion values far away from the equilibrium value, the apparent activation energy of different catalysts can be calculated. Figure 9 shows Arrhenius-type plots for the rates of  $\text{NH}_3$  decomposition reaction over  $x\%$ Ru/c-MgO-DP, 5%Ru/MgO-DP, 5% Ru/ $\text{Al}_2\text{O}_3$ -DP, and 5%Ru/ $\text{SiO}_2$ -DP catalysts. Correlating well with the catalytic activity results, a remarkable decrease in the apparent activation energy can be observed for 5%Ru/c-MgO-DP catalyst in comparison with that of the Ru-based catalysts from metal oxide supports. The apparent activation energy of 5%Ru/c-MgO-DP is 67.3 kJ/mol, which is smaller than that of 5%Ru/MgO-DP (85.0 kJ/mol), 5% Ru/ $\text{Al}_2\text{O}_3$ -DP (88.2 kJ/mol) and 5%Ru/ $\text{SiO}_2$ -DP (104.3 kJ/mol) samples. For the Ru/c-MgO-DP samples with different Ru contents, it can be seen that the  $E_a$  values of Ru/c-MgO-DP decreased obviously with increase of Ru content, which is consistent with our previous results.<sup>[11b]</sup> For different Ru/c-MgO-DP samples, the 5%Ru/c-MgO-DP sample gives a smallest the apparent activation energy. Due to the complex of the supported Ru catalysts, the catalytic performance as well as apparent activation energy of supported Ru catalysts can be influenced by many different factors such as the surface area of support, Ru dispersion, Ru particle size and morphology, interaction between Ru and support, and basic property of support. Here, for the Ru/c-MgO-DP samples with similar surface area, the highly dispersed Ru nanoparticles, high density of basic sites, and strong interaction between Ru nanoparticles and c-MgO may all responsible for the decrease of  $E_a$  values with increase of Ru content.

#### Effect of KOH as modifying agent for 3%Ru/c-MgO-DP catalyst

For  $\text{NH}_3$  decomposition reaction, the rate-determining step is the associative desorption of nitrogen atoms from the catalyst surface. Alkali or alkaline earth ions have been demonstrated as efficient promoters for supported Ru or Fe catalysts due to the electron donation effect.<sup>[4a, 13]</sup> In this work, KOH was applied as the promoter to modify the reduced 3%Ru/c-MgO-DP catalyst. As shown in Figure 10a, KOH modification has an obvious influence on the catalytic performance of 3%Ru/c-MgO-DP catalyst. The  $\text{NH}_3$  conversions of K-3%Ru/c-MgO-DP (K/Ru=1/3) and K-3%Ru/c-MgO-DP (K/Ru=1/2) show an obvious increase in comparison with that of the pristine 3%Ru/c-MgO-DP at temperature above 400°C. The  $\text{NH}_3$  conversion over K-3%Ru/c-MgO-DP (K/Ru=1/2) can reach 96.6% at 475°C, which is much higher than that of the pristine 3%Ru/c-MgO-DP (87.1%). The  $\text{NH}_3$  conversion over K-3%Ru/c-MgO-DP (K/Ru=1/3) is 95.6% at 475°C, which is similar with that of the K-3%Ru/c-MgO-DP (K/Ru=1/2). The KOH modification of Ru/c-MgO-DP has an optimum K/Ru molar ratio. Further increase of K/Ru molar ratio from 1/2 to 1/1 resulted with a remarkably decrease of catalytic activity in the temperature range from 300-500°C. The decrease of activity of K-3%Ru/c-MgO-DP (K/Ru=1/1) should result from the covering of Ru sites with excess of KOH species, which have been often observed for the alkali modified Ru/CNT catalyst.<sup>[4a]</sup>

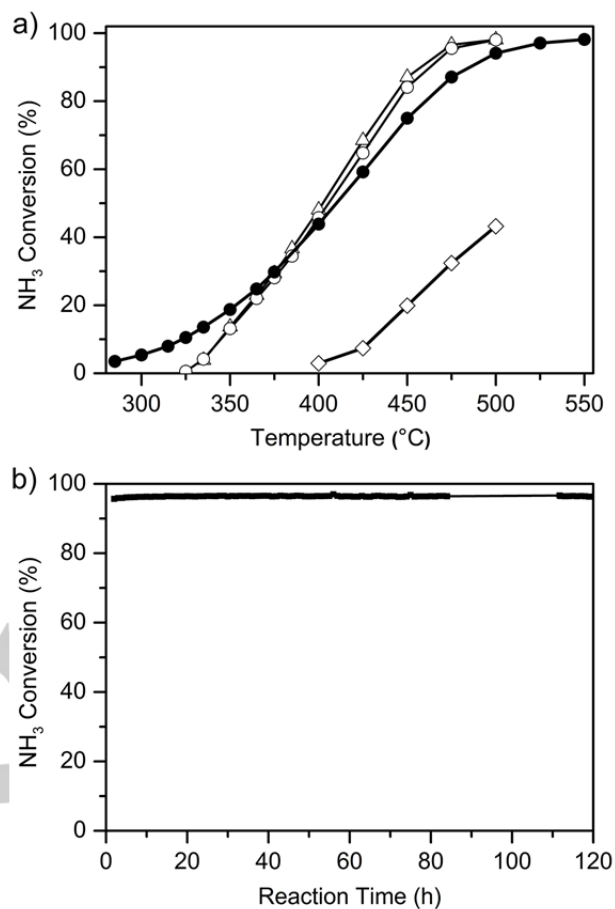


**Figure 10.** (a)  $\text{NH}_3$  conversion as a function of reaction temperature over 3%Ru/c-MgO-DP and KOH modified 3%Ru/c-MgO-DP catalysts: 3%Ru/c-MgO-DP (●); K-3%Ru/c-MgO-DP (K/Ru=1/3) (○); K-3%Ru/c-MgO-DP (K/Ru=1/2) (Δ); K-3%Ru/c-MgO-DP (K/Ru=1/1) (◇). (b) Stability of K-3%Ru/c-MgO-DP (K/Ru=1/2) catalyst for  $\text{NH}_3$  decomposition at 475°C.

Besides activity, the durability of the catalysts is another important property in the practical applications. The catalytic performance of the K-3%Ru/c-MgO-DP (K/Ru=1/2) catalyst was also measured in a long term test. Even the 3%Ru/c-MgO-DP catalyst has been fully reduced before KOH modification, the K-3%Ru/c-MgO-DP (K/Ru=1/2) catalyst still need to be activated through exposure to the  $\text{NH}_3$  stream at optimized high temperature. For the K-3%Ru/c-MgO-DP (K/Ru=1/2) catalyst directly tested at 450-475°C, only a very low  $\text{NH}_3$  conversion of 25-30% can be obtained. However, remarkable enhancement of activity at 450°C can be obtained when the catalyst was pre-treated in a  $\text{NH}_3$  flow at temperature of 500-520°C before the activity test. In the following long isothermal test at 475°C, no obvious activity loss is observed and approximately 95.6% of  $\text{NH}_3$  conversion is maintained over 120 hours, demonstrating that the remarkably high stability of the KOH modified catalyst (Figure 10b). The activation temperature is critical for activation of the K-3%Ru/c-MgO-DP (K/Ru=1/2) catalyst, further increase of activation temperature to 550°C results in a much decreased

activity at 450°C (65.2%), which may be related with the partial loss of K species at the high temperature.

## Conclusions

In summary, this work demonstrates that the use of  $4\text{MgCO}_3 \cdot \text{Mg}(\text{OH})_2 \cdot 4\text{H}_2\text{O}$  as support precursor can strongly affect the basic properties of Ru/MgO catalysts as well as their catalytic activities for  $\text{NH}_3$  decomposition. The Ru/ $4\text{MgCO}_3 \cdot \text{Mg}(\text{OH})_2 \cdot 4\text{H}_2\text{O}$  composite derived Ru/c-MgO catalysts can decompose  $\text{NH}_3$  to produce  $\text{CO}_x$ -free  $\text{H}_2$  with high efficiency and robust stability in the long-term runs (over 100 h). Compared to the conventional MgO support, the use of  $4\text{MgCO}_3 \cdot \text{Mg}(\text{OH})_2 \cdot 4\text{H}_2\text{O}$  as support precursor significantly increases the density of basic sites on the surface of Ru/c-MgO catalysts. Meanwhile, the high density of basic sites also has a significant effect on the dispersion of Ru nanoparticles and metal-support interaction. The highly dispersed Ru nanoparticles, high density of basic sites, and strong interaction between Ru nanoparticles and c-MgO all benefit the excellent catalytic performance of Ru/c-MgO catalysts in  $\text{NH}_3$  decomposition. This work confirms the importance of basic properties of Ru/MgO catalysts for  $\text{NH}_3$  decomposition, and which opens opportunity to develop highly efficient catalysts through tuning the basic properties of catalysts.

## Experimental Section

### Reagents

Ruthenium chloride hydrate ( $\text{RuCl}_3 \cdot x\text{H}_2\text{O}$ ) was obtained from Shanghai Tuosi Chemical Co., LTD,  $\text{Mg}(\text{NO}_3)_2 \cdot 6\text{H}_2\text{O}$  was obtained from Tianjin Kemiou Chemical Reagent Co., Ltd.,  $\text{K}_2\text{CO}_3$  was obtained from Sinopharm Chemical Reagent Co., Ltd..

### Preparation of supports

$4\text{MgCO}_3 \cdot \text{Mg}(\text{OH})_2 \cdot 4\text{H}_2\text{O}$  precursor was prepared by precipitation method.  $\text{Mg}(\text{NO}_3)_2 \cdot 6\text{H}_2\text{O}$  (0.7 mol, 0.4 mol/L) aqueous solution was mixed with  $\text{K}_2\text{CO}_3$  (0.7 mol, 0.4 mol/L) aqueous solution, stir violently for 1 hour at 15°C. The product was obtained by filtration to separate the precipitate from the solution, and then washed for three times with deionized water. Finally, the product was dried at 80°C for 6 h. XRD pattern of the obtained product according well with the standard  $4\text{MgCO}_3 \cdot \text{Mg}(\text{OH})_2 \cdot 4\text{H}_2\text{O}$  (Figure S1).

### Preparation of Ru/c-MgO-DP

The Ru/c-MgO catalyst with Ru loading of 5.0 wt.% was prepared by deposition-precipitation method (DP) according to our previous report.  $\text{RuCl}_3 \cdot x\text{H}_2\text{O}$  (0.5 g Ru, 0.5 g/L) aqueous solution was first mixed with 22.2 g of  $4\text{MgCO}_3 \cdot \text{Mg}(\text{OH})_2 \cdot 4\text{H}_2\text{O}$  powder. Subsequently, a designated amount of urea with a molar ratio of Ru to urea at 1:200 was added as the precipitation agent. The mixture was reacted at 80°C for 8 h and aged at room temperature for 12 h. The product was obtained by filtration to separate the precipitate from the solution, and then washed for three times with deionized water. Finally, the product was dried at 80°C for 6 h. To evaluate the effect of ruthenium content on catalyst, we've prepared a series of the catalysts, identified as x%Ru/c-MgO-DP, where x corresponding to the weight percent of Ru metal in the catalysts.

To evaluate the effect of DP method on the structure and performance of the different supports, Ru/MgO-DP, Ru/ $\text{Al}_2\text{O}_3$  and Ru/ $\text{SiO}_2$  with Ru loading of 5 wt.% prepared by DP method and tested in  $\text{NH}_3$  decomposition. MgO powder was purchased from Shenyang chemical reagent plant, China. To compare the influence of DP method and incipient wetness impregnation on the catalytic performance, 5%Ru/c-MgO-IM sample prepared by incipient wetness impregnation. The concentration of  $\text{RuCl}_3 \cdot x\text{H}_2\text{O}$  was 25 mg/mL. The acetone solution was added to the  $4\text{MgCO}_3 \cdot \text{Mg}(\text{OH})_2 \cdot 4\text{H}_2\text{O}$  support, and then the solvent was removed in air to obtain the air-dry sample. Subsequently, the sample was dried at 80°C for another 2 h. After that, the sample was heated in flowing Ar to 550°C for 2 h.

The as-prepared 3%Ru/c-MgO-DP sample was reduced in flowing  $\text{NH}_3$  at 550°C for 2 h. Then KOH promoter was loaded onto the reduced 3%Ru/c-MgO-DP sample by incipient wetness impregnation from the ethanol solution of KOH. The sample was dried at 80°C for overnight, and the obtained KOH modified 3%Ru/c-MgO-DP catalyst was denoted as K-3%Ru/c-MgO-DP.

### Characterization

The Ru metal loading in Ru/c-MgO-DP sample was determined by inductively coupled plasma-atomic emission spectroscopy (ICP-AES, Optima 2000DV, USA). XRD patterns were recorded on an X'Pert Pro (PANalytical) diffractometer with  $\text{Cu K}_\alpha$  radiation ( $\lambda = 0.1542 \text{ nm}$ ) at 40 kV and 40 mA. The contents of residual chlorine in the prepared catalysts were determined on a PANalytical Zetium X-ray fluorescent spectrometer.

Nitrogen adsorption/desorption isotherms were undertaken isothermally at -196°C with a Micromeritics ASAP 2020 analyzer. The samples were degassed at 300°C and  $10^{-3} \text{ Pa}$  for at least 8 h before the measurements. The surface areas are determined by applying the Brunauer-Emmett-Teller (BET) method in the relative pressure range of 0.05-0.25. The pore volume is calculated at the relative pressure of 0.99.

$\text{CO}_2$ -TPD measurements were conducted on a Micromeritics 2920 apparatus. In a typical  $\text{CO}_2$ -TPD experiment, the sample was activated in a flow of He (99.999%) at a rate of 10°C/min to 400°C and kept at 400°C for 2 h prior to the adsorption of  $\text{CO}_2$  at 100°C. After purging the physically adsorbed  $\text{CO}_2$  at 100°C with He, the sample was heated to 900°C at a rate of 10°C/min, and the  $\text{CO}_2$  liberated was detected by a chromatograph equipped with thermal conductivity detector to determine the amount of  $\text{CO}_2$  desorbed from the catalysts.

Thermogravimetric Analysis-Differential Thermal Analysis (TG-DTA) measurements were carried out on a Netzsch STA449C thermal analysis system. A heating rate of 2 C/min was applied to 5 mg sample.  $\text{H}_2$ -TPR was operated in a home-made apparatus. Prior to each measurement, the sample (0.1 g) was heated from room temperature to 450°C with a heating rate of 5°C/min under Ar flow (30 mL/min), and kept at 450°C for 120 min. After being cooled to room temperature, the gas flow was switched to 5%  $\text{H}_2/\text{Ar}$  (30 mL/min) and reduced the sample with a temperature ramp of 10°C/min. The TPR profiles were measured with a gas chromatograph equipped with thermal conductivity (TCD) detector. The reducibility of the loaded metal component was estimated based on the extent of  $\text{H}_2$  consumption.

The morphologic characterization was performed on a JEOL 2100X transmission electron microscope operating at 200 kV. In order to obtain suitable samples, the catalyst powders were dispersed in ethanol by ultrasonic and then a drop of the solution was placed on a carbon-coated copper grid.

The exposed Ru surface area was measured by CO pulse chemisorption using an automated chemisorption analysis instrument from Altamira (AMI-200). The catalyst was loaded into a 1/4 inch quartz tube for each test. Prior to the pulse CO chemisorption measurement, Prior to the pulse CO chemisorption measurement, the catalyst was reduced at 400°C for 2 h in 10%  $\text{H}_2/\text{Ar}$ , and then cooled down to room temperature in He. CO pulses were introduced to the sample (250 mL of

pure CO) and the CO uptake was measured using a gas chromatography equipped with TCD detector. The Ru dispersion was calculated by assuming a CO:Ru stoichiometry of 1:1.

#### Catalytic performance measurement

Catalytic tests were carried out on a continuous fixed-bed flow quartz reactor (catalyst: 50 mg, 20-40 mesh) under atmospheric pressure with a pure NH<sub>3</sub> gas hour space velocity (GHSV) of 30,000 mL/g<sub>cat</sub>·h. Prior to the reaction, the dried catalysts (20-60 mesh) were heated in an NH<sub>3</sub> flow (25 mL/min) from room temperature to 550°C at a heating rate of 5°C/min. Reduced catalysts could be obtained after reduction in a NH<sub>3</sub> flow at 550°C for 2 h. All the activity tests of catalysts were conducted under atmospheric pressure, and pure NH<sub>3</sub> was used as the only reactant. The reaction temperature was in the range of 285-550°C. Product gas composition was analyzed by on-line gas chromatograph (GC-7890, Agilent) equipped with a thermal conductivity detector and Porapak N column with H<sub>2</sub> as carrier gas.

#### Acknowledgements

This work is financially supported by the Sino-Japanese Research Cooperative Program of Ministry of science and technology (2016YFE0118300), projects National Natural Science Foundation of China (21633011), and the DICP DMTO program (DICPDMTO201504).

**Keywords:** Ru/MgO catalyst • Ru/4MgCO<sub>3</sub>·Mg(OH)<sub>2</sub>·4H<sub>2</sub>O composite • CO<sub>x</sub>-free H<sub>2</sub> • ammonia decomposition • basic sites

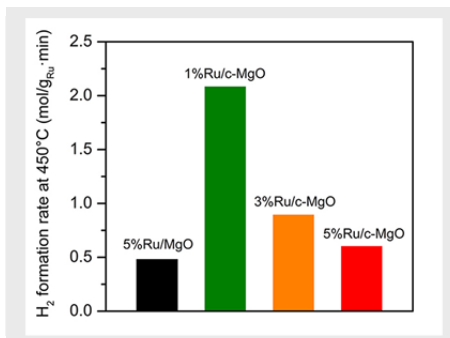
- [1] T. He, P. Pachfule, H. Wu, Q. Xu, P. Chen, *Nat. Rev. Mater.* **2016**, *1*, 17.
- [2] aA. Klerke, C. H. Christensen, J. K. Nørskov, T. Vegge, *Journal of Materials Chemistry* **2008**, *18*, 2304-2310; bR. Lan, J. T. S. Irvine, S. W. Tao, *Int. J. Hydrog. Energy* **2012**, *37*, 1482-1494; cR. Metkemeijer, P. Achard, *Int. J. Hydrog. Energy* **1994**, *19*, 535-542.
- [3] aB. L. Yi, *Technology and Application, Chemical Industry Press, Beijing* **2003**, *2*; bR. O. Idem, N. N. Bakhshi, *Ind Eng Chem Res* **1994**, *33*, 2047-2055; cA. S. Chellappa, C. M. Fischer, W. J. Thomson, *Appl Catal a-Gen* **2002**, *227*, 231-240; dT. V. Choudhary, D. W. Goodman, *Catal Lett* **1999**, *59*, 93-94; eV. R. Choudhary, B. S. Uphade, A. S. Mamman, *J Catal* **1997**, *172*, 281-293; fJ. N. Armor, *Appl Catal a-Gen* **1999**, *176*, 159-176; gT. V. Choudhary, C. Sivadinarayana, D. W. Goodman, *Catal Lett* **2001**, *72*, 197-201; hM. E. E. Abashar, Y. S. Al-Sughair, I. S. Al-Mutaz, *Appl Catal a-Gen* **2002**, *236*, 35-53; iS. F. Yin, B. Q. Xu, C. F. Ng, C. T. Au, *Appl Catal B-Environ* **2004**, *48*, 237-241; js. F. Yin, Q. H. Zhang, B. Q. Xu, W. X. Zhu, C. F. Ng, C. T. Au, *J Catal* **2004**, *224*, 384-396.
- [4] aS. F. Yin, B. Q. Xu, S. J. Wang, C. F. Ng, C. T. Au, *Catal Lett* **2004**, *96*, 113-116; bJ. C. Ganley, F. S. Thomas, E. G. Seebauer, R. I. Masel, *Catal Lett* **2004**, *96*, 117-122.
- [5] aY. X. Li, L. H. Yao, Y. Y. Song, S. Q. Liu, J. Zhao, W. J. Ji, C. T. Au, *Chem Commun* **2010**, *46*, 5298-5300; bX. K. Li, W. J. Ji, J. Zhao, S. J. Wang, C. T. Au, *J Catal* **2005**, *236*, 181-189.
- [6] aG. Li, M. Kanezashi, T. Tsuru, *Catal Commun* **2011**, *15*, 60-63; bJ. Okal, M. Zawadzki, L. Kepinski, L. Krajczyk, W. Tylus, *Appl Catal a-Gen* **2007**, *319*, 202-209.
- [7] Y. V. Larichev, *J Phys Chem C* **2011**, *115*, 631-635.
- [8] L. Li, Z. H. Zhu, Z. F. Yan, G. Q. Lu, L. Rintoul, *Appl Catal a-Gen* **2007**, *320*, 166-172.
- [9] aF. R. Garcia-Garcia, J. Alvarez-Rodriguez, I. Rodriguez-Ramos, A. Guerrero-Ruiz, *Carbon* **2010**, *48*, 267-276; bF. Chang, J. P. Guo, G. T. Wu, L. Liu, M. Zhang, T. He, P. K. Wang, P. Yu, P. Chen, *Rsc Adv* **2015**, *5*, 3605-3610.
- [10] F. Hayashi, Y. Toda, Y. Kanie, M. Kitano, Y. Inoue, T. Yokoyama, M. Hara, H. Hosono, *Chem. Sci.* **2013**, *4*, 3124-3130.
- [11] aJ. Zhang, H. Y. Xu, Q. J. Ge, W. Z. Li, *Catal Commun* **2006**, *7*, 148-152; bX. H. Ju, L. Liu, P. Yu, J. P. Guo, X. L. Zhang, T. He, G. T. Wu, P. Chen, *Appl Catal B-Environ* **2017**, *211*, 167-175.
- [12] aS. Murata, K. Aika, *J Catal* **1992**, *136*, 110-117; bC. H. Liang, Z. B. Wei, Q. Xin, C. Li, *Appl Catal a-Gen* **2001**, *208*, 193-201; cA. M. Karim, V. Prasad, G. Mpourmpakis, W. W. Lonergan, A. I. Frenkel, J. G. G. Chen, D. G. Vlachos, *J. Am. Chem. Soc.* **2009**, *131*, 12230-12239.
- [13] Z. Kowalczyk, S. Jodzis, W. Rarog, J. Zielinski, J. Pielaszek, *Appl Catal a-Gen* **1998**, *173*, 153-160.

Entry for the Table of Contents (Please choose one layout)

Layout 1:

## FULL PAPER

**NH<sub>3</sub>-to-H<sub>2</sub>:** The Ru/c-MgO catalysts derived from Ru/4MgCO<sub>3</sub>·Mg(OH)<sub>2</sub>·4H<sub>2</sub>O which have high density of basic sites and enhanced Ru dispersion show excellent catalytic activity and stability in NH<sub>3</sub> decomposition.



Xiaohua Ju, Lin Liu,\* Xilun Zhang, Ji Feng, Teng He, Ping Chen\*

Page No. – Page No.

**Highly Efficient Ru/MgO Catalyst with Surface-Enriched Basic Sites for Production of Hydrogen from Ammonia Decomposition**